Available online at www.sciencedirect.com
ScienceDirect
Lithos 93 (2007) 328–339
LITHOS
www.elsevier.com/locate/lithos

The Serra da Graciosa A-type Granites and Syenites, southern Brazil Part 3: Magmatic evolution and post-magmatic breakdown of amphiboles of the alkaline association

Guilherme A.R. Gualda *, Silvio R.F. Vlach

Departamento de Mineralogia e Geotectônica, Instituto de Geociências, Universidade de São Paulo, Rua do Lago, 562, Cidade Universitária, 05508-080, São Paulo, SP, Brazil

Received 31 January 2005; accepted 1 May 2006
Available online 30 August 2006

Abstract

Amphiboles are the main mafic minerals in most metaluminous to peralkaline alkali-feldspar granites and syenites, and they usually preserve an important record of the compositional evolution of the melts from which they crystallize. In the alkaline association of the Serra da Graciosa A-type Granites and Syenites (southern Brazil), amphibole compositions span a large range, including calcic, sodic–calcic, and sodic amphiboles. Calcic amphiboles are typically observed in the metaluminous rocks, while sodic amphiboles are characteristic of the more strongly peralkaline rocks; sodic–calcic amphiboles are found in intermediate varieties. Compositional variations record the differentiation trends within two petrographic series of the alkaline association. The overall evolution of amphibole compositions is similar in both: they reveal a progressive increase in Na and Fe^{3+} with differentiation (increase in alkalinity of the magmas), a characteristic shared by undersaturated peralkaline (or agpaitic) differentiation trends. In detail, however, the evolutions of the amphibole compositions in the two series are distinct. In Alkaline series 1, the cores of the crystals form a continuum from calcic to sodic compositions, with the exception of a small compositional gap within the sodic–calcic amphiboles. The rims, however, show compositions that diverge from this main trend; this divergence results from increasing amounts of the oxy-amphibole component, and reflects more oxidizing conditions at the final stages of magmatic crystallization. In Alkaline series 2, these oxidation trends are much more subtle and a reverse trend is observed in the sodic amphiboles. Sodic–calcic amphiboles are in several cases replaced by intergrowths of post-magmatic sodic amphibole and Al-poor ("tetrasilicic") biotite.
© 2006 Elsevier B.V. All rights reserved.

Keywords: A-type rocks; Amphibole; Petrography; Microscopy and microanalysis; Serra da Graciosa; Brazil

1. Introduction

Amphiboles are important mafic minerals in most intermediate to acid igneous rocks, in particular in granitic and syenitic rocks (Deer et al., 1992, 1997). Because of the extensive compositional variability of natural amphiboles, they constitute important records of the chemical evolution of the melts from which they crystallized. In particular, compositional variations of amphiboles (1) reflect the degree of alumina saturation of the magma (Shand, 1972; Carmichael et al., 1974; Giret et al., 1980), (2) influence the silica saturation of crystallizing melts (Giret et al., 1980), and (3) record the oxidation state of the

* Corresponding author. Current address. Department of the Geophysical Sciences, The University of Chicago, 5734 S. Ellis Ave., Chicago, IL 60637, USA. Tel.: +1 773 702 8101; fax: +1 773 702-9505.
E-mail address: ggualda@uchicago.edu (G.A.R. Gualda).

0024-4937/$ - see front matter © 2006 Elsevier B.V. All rights reserved.
doi:10.1016/j.lithos.2006.03.070

solidifying magma (Strong and Taylor, 1984). The study of amphiboles can thus yield fundamental information about magmatic evolution and differentiation.

This is particularly the case for A-type granites and syenites, which show a large range of compositions in terms of alumina saturation (see Pitcher, 1997 and references therein). A-type granites and syenites include metaluminous to mildly peraluminous granitic rocks of the aluminous association (King et al., 1997) and also metaluminous to peralkaline syenites and granites of the alkaline association (for a discussion, see Gualda and Vlach, 2007-this issue). Because of pronounced variation in alumina saturation, amphiboles are particularly useful in deciphering the paths of magmatic evolution in A-type granites associations.

Amphiboles in A-type and alkaline undersaturated rocks have been studied in detail by many authors (Barker et al., 1975; Neumann, 1976; Giret et al., 1980; Della Ventura et al., 2005; Strong and Taylor, 1984; Hoshino, 1986; Platt and Woolley, 1986; Czamanske and Dillet, 1988; Woolley and Jones, 1992; Njonfang and Moreau, 2000; Marks et al., 2003). Giret et al. (1980) showed that amphiboles grade from calcic to sodic–calcic and sodic with increasing alkalinity clearly demonstrating how amphibole compositions reflect the alkalinity of the environment in which they crystallize. Furthermore, because calcic amphiboles in these rocks contain less silica than the melt from which they crystallize, amphibole crystallization frequently leads to magmas that are progressively more silica saturated (Giret et al., 1980). Additionally, Strong and Taylor (1984) have argued that, under oxidizing conditions, amphiboles tend to favor the oxy-amphibole substitutions, so that amphibole composition can also be used as qualitative indicators of the degree of oxidation of magmas. Overall, a considerable amount of data has accumulated for amphiboles from granitic rocks (for a review, see Deer et al., 1997, pp. 434–445, 629–631), and it is clear that series from different localities are characterized by distinct crystallization histories.

This contribution is part of a series of papers detailing the mineralogy and petrography of the Serra da Graciosa Granites and Syenites, southern Brazil (Gualda and Vlach, submitted for publication). Amphibole is the main mafic mineral in the Serra da Graciosa alkaline petrographic series (Gualda and Vlach, 2007-this issue), and the evolution of amphiboles is distinctive and characteristic of each individual petrographic series. The compositional variations observed within each petrographic series are extreme, and encompass the full spectrum of variability reported worldwide (Giret et al., 1980; Strong and Taylor, 1984; Platt and Woolley, 1986; see also Deer et al., 1997). By combining compositional variation with textural features, we model amphibole crystallization from the early-magmatic stage to the late-magmatic stage in Serra da Graciosa. We also discuss the importance of post-magmatic (i.e., subsolidus) destabilization of sodic–calcic amphiboles (Giret et al., 1980) and crystallization of sodic amphiboles (Hoshino, 1986) in association with Al-poor biotite (Czamanske and Dillet, 1988).

2. Local geology

The Serra da Graciosa Granites and Syenites comprise five closely spaced granitic and syenitic plutons in the Graciosa A-type Province in southern Brazil, formed during the final stages of the Brasiliano/Pan-African orogeny at 580–600 Ma (Kaul and Cordani, 2000; Siga et al., 1993). Six petrographic series were recognized by Gualda and Vlach (2007-this issue), three of them of alkaline affinity (Alkaline series 1, 2, and 3 — the alkaline association), two of aluminous affinity (Aluminous series 1 and 2 — the aluminous association), and one including monzodiorites and other associated granitoids. The mafic minerals present are, in general, Fe-rich and low in Mg and Al. In the aluminous association, the amphiboles are calcic and rather homogeneous. In the monzodioritic rocks, amphiboles are also homogeneous, but are distinctively more Mg-rich. In Alkaline series 3, only two petrographic varieties are observed, only one of which is amphibole-bearing. This contribution will be limited to Alkaline series 1 and Alkaline series 2 (for details, see Gualda and Vlach, 2007-this issue, submitted for publication).

Alkaline series 1 is composed of predominant alkali-feldspar syenites and subordinate alkali-feldspar granites. In the quartz-poor members of this series, calcic amphibole, hedenbergitic clinopyroxene and olivine are the main mafic phases, and allanite is an important accessory mineral. With increasing quartz content, olivine disappears, clinopyroxene becomes more Fe-rich and less abundant, and sodic–calcic amphibole becomes the main mafic phase; chevkinite–perrierite appears instead of allanite in these rocks. In the most evolved alkali-feldspar granites, no clinopyroxene is present and primary sodic amphibole is observed (Gualda and Vlach, 2007-this issue).

Alkaline series 2 includes rocks texturally distinct from those of Alkaline series 1. Modal variations are very restricted in this series, with all varieties corresponding to alkali-feldspar granites with amphibole as the sole mafic mineral. Amphibole compositions are also quite varying, from calcic to sodic–calcic and sodic. This variation is accompanied by a change in the accessory mineralogy, with allanite as the main accessory phase in

rocks with calcic amphibole, and chevkinite–perrierite in those with sodic–calcic and sodic amphibole (Gualda and Vlach, 2007-this issue). The geology and petrography of the Serra da Graciosa Granites and Syenites are described in more detail in our companion paper (Gualda and Vlach, 2007-this issue). Gualda and Vlach (submitted for publication) present a geological map of the plutons, including the location of sampled outcrops.

3. Methods

Compositional point analyses and scanning electron microscopy images were obtained using a JEOL JXA-8600S microprobe at the Instituto de Geociências, Universidade de São Paulo, equipped with 5 wavelength-dispersive spectrometers and 1 energy-dispersive spectrometer. Back-scattered electron (BSE) images were used to characterize in detail the zoning patterns verified using optical microscopy (e.g., based on variations of pleochroic pattern and extinction angle), with beam conditions of 15 kV, 20 nA and 1 μm. Quantitative WDS analyses were performed along core–rim profiles to fully characterize the variations present in each sample. Beam conditions were 15 kV, 20 nA and 5 μm for both amphibole and biotite. Maximum pulse integration times were between 10 and 80 s. Matrix effects were corrected using the PROZA procedure (Bastin and Heijligers, 1990). Both natural and synthetic compounds were used as standards. Analytical conditions employed are summarized in Appendix A. Estimated maximum total errors (2σ) are below 1% and 5% for major and minor elements, respectively, but are greater than 10% for some trace elements with concentrations close to the detection limits. The quality of the analyses was checked by occasionally analyzing Arenal and Kakanui hornblende standards (Jarosewich et al., 1980).

Mineral formulae were calculated using the program Mincal developed by us. In the case of amphiboles, Fe^{2+} and Fe^{3+} were estimated from total Fe following the procedure suggested by Gualda and Vlach (2005), a variant of the method of Schumacher (1997), which uses the maximum Fe^{3+} estimates instead of average between maximum and minimum estimates as originally recommended by Schumacher. For biotite, all Fe is presented as Fe^{2+}, and formulae were calculated based on 22 oxygen ions.

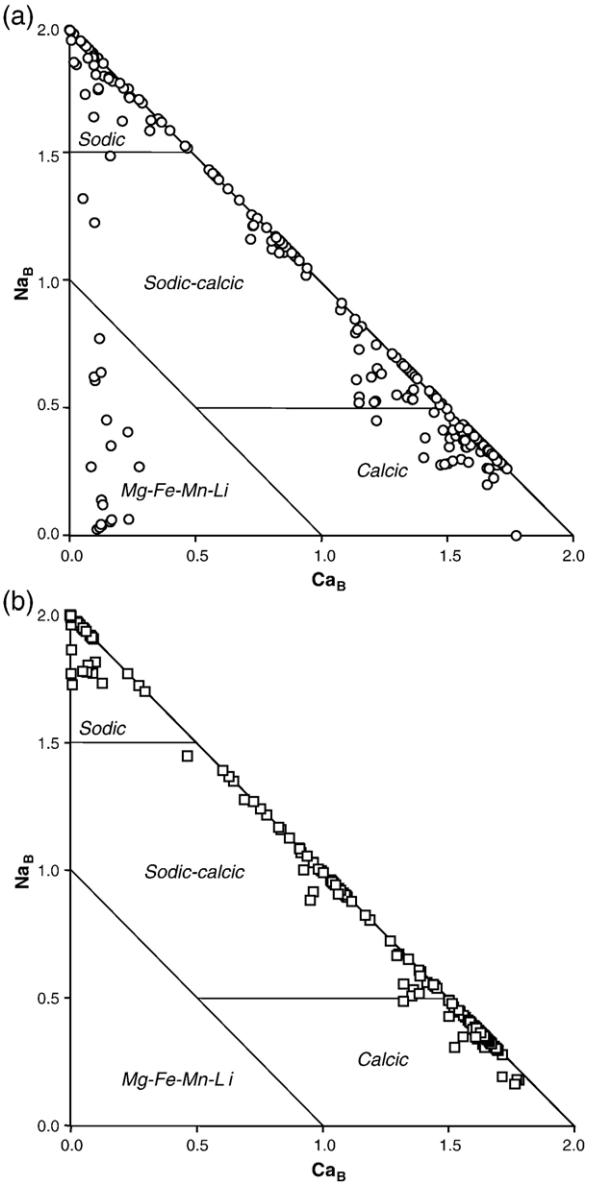


Fig. 1. Ca_B–Na_B cationic plots showing amphibole compositions for (a) Alkaline series 1 and (b) Alkaline series 2 of the Serra da Graciosa A-type Granites and Syenites. Notice the full spectrum of compositions, from calcic to sodic–calcic and sodic; boundaries between fields according to Leake et al. (1997). In (a), the trend from Mg–Fe–Mn–Li amphiboles towards sodic compositions corresponds to secondary grunerite (probably by Na loss at relatively low temperatures).

4. Results

4.1. Amphibole

Amphiboles in the alkaline association of the Serra da Graciosa Granites and Syenites span from calcic to sodic varieties (Fig. 1; Appendix B). The calcic amphiboles are typically ferrohornblende and ferro-edenite, and subordinately ferro-actinolite. The sodic–calcic varieties are mostly ferrobarroisite and ferrowinchite, with subordinate amounts of ferrorichterite and katophorite. The sodic amphiboles are mostly riebeckite, and rarely arfvedsonite. Secondary Fe–Mg–Mn amphibole (typically grunerite) after olivine is observed in some of the rocks.

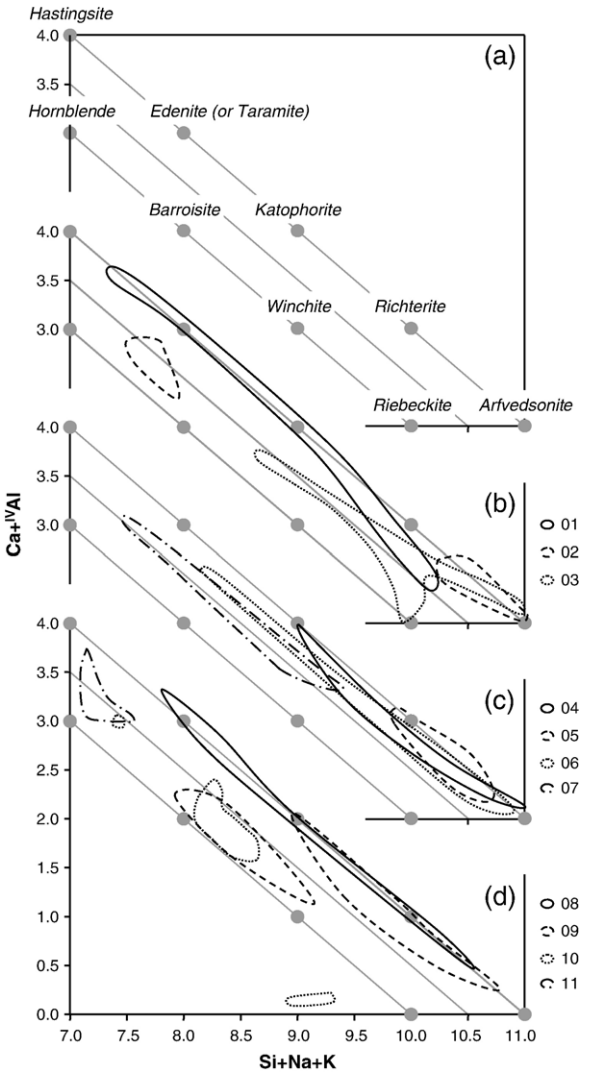


Fig. 2. (Si+Na+K) vs. (Ca+^{IV}Al) cationic plots (after Giret et al., 1980) showing the compositional variation of amphiboles from various localities. In (a), the names of ideal amphibole end-members are shown. End-members with the A position completely vacant fall on the line of slope-1 with the sum of variables at 10; end-members with the A position completely filled fall along the line with the sum of variables at 11. In (b), (c), and (d), compositional trends reported in various studies are portrayed. All these data were recalculated using the program Mincal developed by us using the method of Schumacher (1997) as modified by Gualda and Vlach (2005). Names and references for the localities are: 1 — Oslo rift, undersaturated rocks (Neumann, 1976); 2 — Oslo rift, oversaturated rocks (Neumann, 1976); 3 — Newfoundland (Strong and Taylor, 1984); 4 — Mulanje (Platt and Woolley, 1986); 5 — Pandé (Njonfang and Moreau, 2000); 6 — Puklen (Marks et al., 2003); 7 — Zomba-Malosa (Woolley and Jones, 1992); 8 — Klokken (Parsons, 1981); 9 — Rallier-du-Baty (Giret et al., 1980); 10 — Cauro Bastelica (Giret et al., 1980); 11 — Iskou (Giret et al., 1980).

The compositional variation in calcic to sodic amphiboles can be examined in diagrams like those in Figs. 2 and 3. These can be used for amphiboles with the B position occupied only by Na and Ca (i.e., all but Fe–Mg–Mn amphiboles). For these, the sum of the variables Ca, ^{IV}Al, Si, Na, K corresponds to the sum of the cations in the A, B and T positions. As the sum of B and T equals 10 cations, amphiboles with the A position vacant fall along the lower line in Fig. 2, while

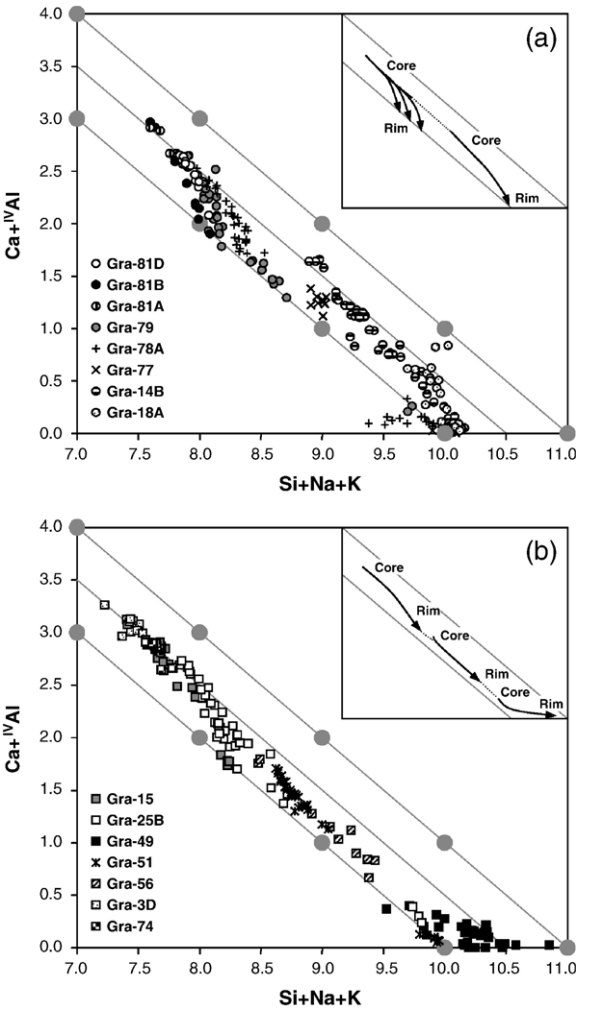


Fig. 3. (Si+Na+K) vs. (Ca+^{IV}Al) cationic plots (after Giret et al., 1980) showing the compositional evolution of amphiboles of the Serra da Graciosa Granites and Syenites. Most of the compositions obtained fall along or close to a line of equal sum 10.5. The rims of many amphibole crystals in Alkaline series 1 (a) deviate from this main trend, which can be explained by an increasingly oxidizing environment. The sodic–calcic amphiboles in Alkaline series 2 (b) lack this oxidizing trend and show sums significantly below 10.5. Different symbols correspond to distinct samples, as indicated in the legend; in the text, samples are referred simply by their numbers.

amphiboles with the A position completely full fall along the upper line in Fig. 2. In Fig. 2b–d, compositional trends of amphiboles from several localities worldwide are illustrated. Fig. 2 shows that amphibole compositions occupy most of the compositional space represented in these diagrams, and that individual localities are characterized by varied compositional trends.

Variation in amphibole compositions in the Serra da Graciosa Granites and Syenites (Fig. 3) is extreme compared to most of the occurrences shown in Fig. 2. Both associations from Serra da Graciosa have compositions that span the full spectrum from calcic to sodic amphiboles (cf. Giret et al., 1980; Strong and Taylor, 1984; Platt and Woolley, 1986; see also Deer et al., 1997). Importantly, the trends observed are not paralleled by those found elsewhere. Because the trends for the Alkaline 1 and Alkaline 2 series are somewhat different from each other, they are described separately below.

4.1.1. Alkaline series 1

A complete gradation from calcic to sodic amphiboles is seen in the Alkaline series 1 (Figs. 1a and 3a). This variation is accompanied by variations in the modal composition of the host rocks, with calcic amphibole in the rocks with least quartz; the gradual increase in quartz abundance is followed by an increase in the amount of Na in the amphiboles (Gualda and Vlach, 2007-this issue).

Amphiboles in this series only rarely form euhedral crystals (Fig. 4a), and more commonly appear as interstitial grains with some developed crystal faces (Fig. 4b–c). In general, the more sodic amphiboles are more clearly interstitial (Fig. 4b), sometimes forming poikilitic crystals. Concentric zoning is common, as illustrated in Fig. 5a (analyses 1–8; location of analytical points in Fig. 4a) and Fig. 5b (analyses 8–15; locations in Fig. 4c).

Despite the gradual nature of the variations, there is a compositional gap between the sodic–calcic and calcic amphiboles (Fig. 3a). This compositional gap clearly divides the amphiboles of this series into two groups. The first one is characterized by calcic and sodic–calcic amphiboles (e.g., samples 81D, 81B, 81A, 78A), while the second group includes sodic and to a lesser extent sodic–calcic compositions (samples 14B, 18A). In both cases, the compositional variations are recorded as gradual concentric zoning patterns (Fig. 5a–b). In general, the variations are more pronounced in the sodic–calcic and sodic amphiboles (e.g., sample 14B; Figs. 4a, b, 5a). In both groups, the cores of the grains have relatively homogeneous compositions, with the A position nearly half-filled (Fig. 5a, b). Toward the rims, the compositions are more sodic with a simultaneous decrease in the sum $(Na+K)_A$. As a result, the core compositions fall along the intermediate line in Fig. 3a (sum of variables 10.5), while the rim compositions gradually converge to the lower line (sum of variables 10.0). The more sodic the core, the more sodic the rims and thus the evolution of the rims towards decreasing $(Na+K)_A$ values was not so much influenced by the alkalinity of the magma. It is also noteworthy that the evolution of Fe^{3+} parallels that of Na_B. The compositional gap separating the two groups of samples (Fig. 3a) is also reflected in the [Na+K]/Al ratio (Fig. 6a) that it reflects the degree of alumina saturation (or alkalinity) of the magma (Giret et al., 1980).

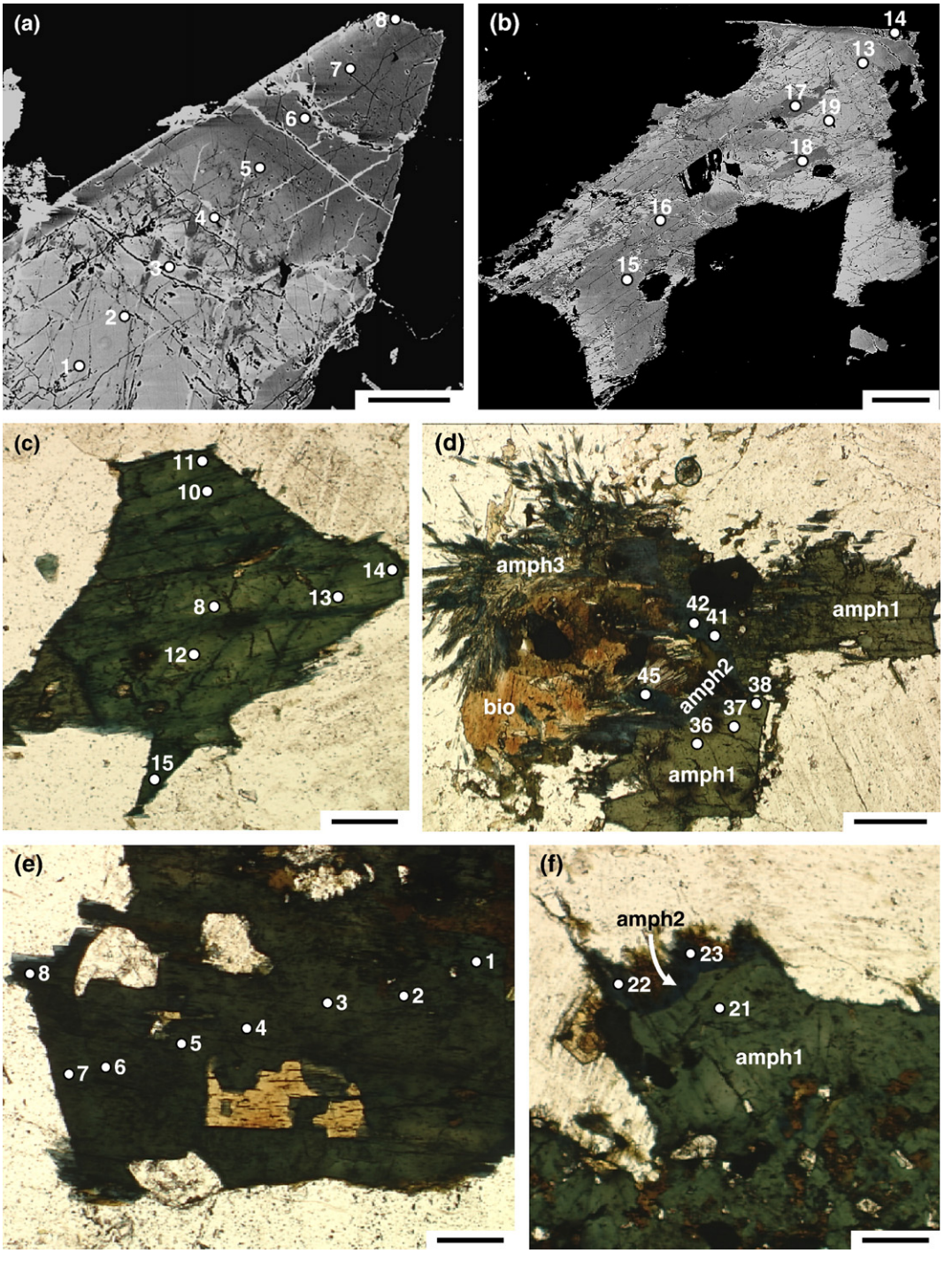
Most of the rocks in this series show evidence for subsolidus equilibration stages of evolution (cf. Hoshino, 1986). These changes are most clearly seen in the formation of exsolution lamellae, occasional development of secondary albite and swapped rims in adjacent alkali feldspar crystals. Importantly, however, the post-magmatic transformations also affect amphiboles. In many cases, the primary amphiboles coexist with riebeckitic amphiboles. Typically, a large compositional gap between the two groups is seen within a given sample (e.g., sample 78A; Fig. 3a). These sodic amphibole crystals are found along fractures and they form overgrowths (spot 14, Figs. 4b and 5a; spots 41–42, Figs. 4d and 5b) or fringes of acicular sodic amphibole (spot 45, Figs. 4d and 5b) in contact with primary calcic or

Fig. 4. Back-scattered electron images (a, b) and photomicrographs (c–f) showing amphibole textures. (a) Euhedral amphibole crystal in sample 14B (Alkaline series 1), which grades from sodic–calcic in the core (light gray) to sodic in the rim (dark gray); bar corresponds to 300 μm. (b) Interstitial amphibole crystal in sample 14B (Alkaline series 1), which shows several distinct zones; compositions of zones indicated by numbers 13, 15, 16, 19 are magmatic, while the others correspond to post-magmatic replacement; bar corresponds to 300 μm. (c) Interstitial sodic–calcic amphibole in sample 78A (Alkaline series 1); bar corresponds to 150 μm. (d) Primary sodic–calcic amphibole crystal in sample 78A (Alkaline series 1) partly replaced by an intergrowth of post-magmatic sodic amphibole and biotite; preserved magmatic portion is to the right and bottom (amph1), an intergrowth of acicular navy-blue sodic amphibole (amph3) and red biotite is seen on the left and top; a zone of blue sodic amphibole (amph2) is found between the two other amphiboles; bar corresponds to 300 μm. (e) Irregular sodic–calcic amphibole in sample 51 (Alkaline series 2), which is characterized by relatively homogeneous compositions; bar corresponds to 150 μm. (f) Fringe of blue sodic amphibole (amph2) developed around primary sodic–calcic amphibole (amph1) in sample 51 (Alkaline series 2); bar corresponds to 150 μm. Plain-polarized light in all photomicrographs. Selected microprobe spots are indicated by white dots and numbers (cf. Fig. 5).

sodic–calcic amphibole, and as irregular domains within primary sodic amphibole (spots 17–18, Figs. 4b and 5a) or as radiating aggregates (Fig. 4d). These aggregates frequently include biotite, and sometimes entirely replace the primary amphibole (Fig. 7a, b, below). Some of the subsolidus amphiboles register loss of Na. They are usually colorless grunerite and show a compositional trend towards Fe–Mg–Mn amphiboles (Fig. 1a).

4.1.2. Alkaline series 2

In Alkaline series 2, amphibole appears as subhedral to irregular crystals, in many respects similar to those



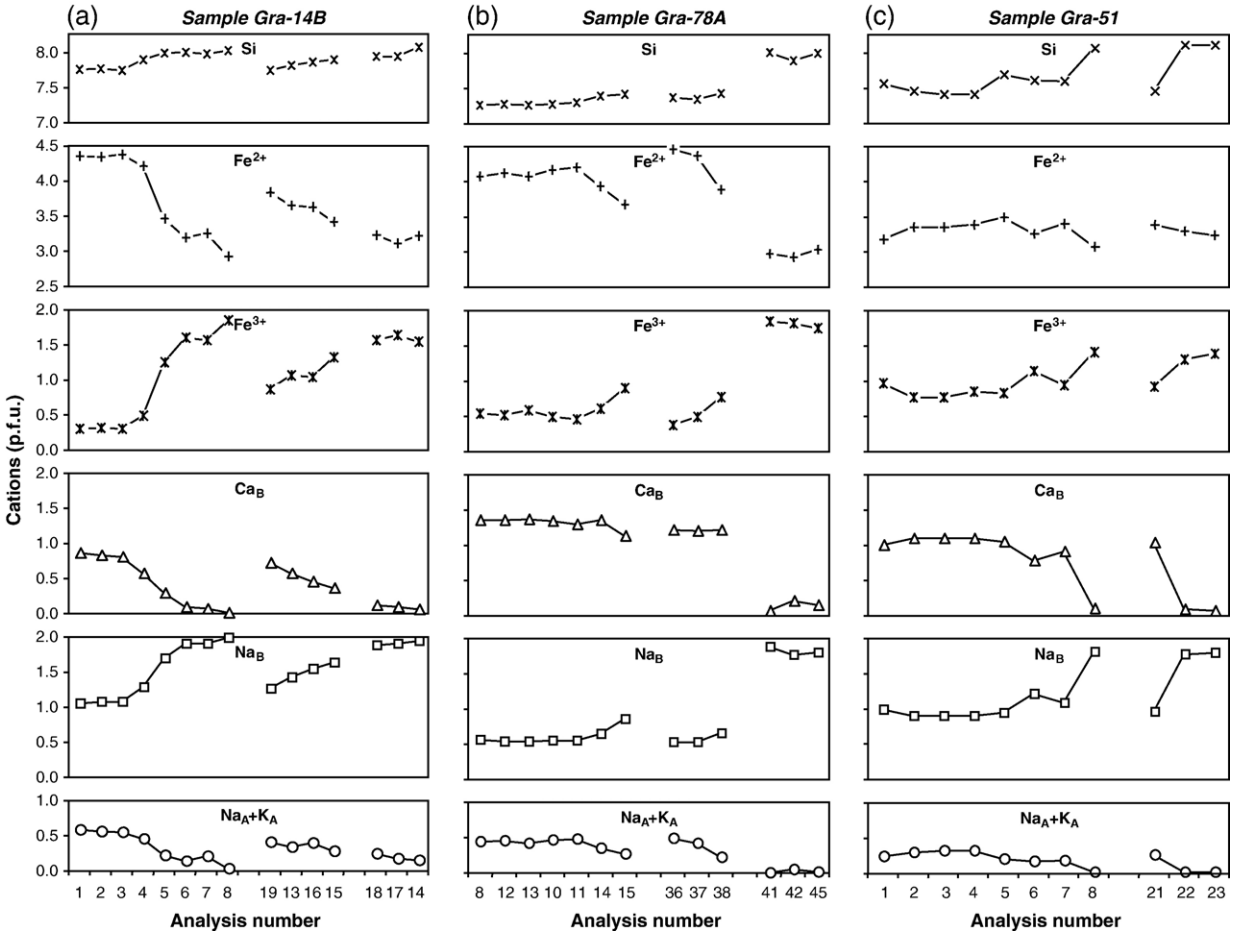


Fig. 5. Compositional variation in selected amphibole crystals in samples (a) 14B (Alkaline series 1), (b) 78A (Alkaline series 1), and (c) 51 (Alkaline series 2). Locations of the spots are shown in Fig. 4.

in Alkaline series 1 (e.g., Fig. 4e). In some of the samples (e.g., 15 and 25B), amphibole crystals are not found uniformly throughout the rock and euhedral crystals are locally present; this is particularly the case for samples with calcic amphibole.

The composition of amphiboles in this series is the only effective indicator of differentiation, as there is little modal variation. Compared to the amphiboles of Alkaline series 1 (Fig. 1b), they show somewhat more elevated mg# values (Appendix B) as well as distinct compositional evolution in detail (Fig. 3b). The more calcic amphiboles (samples 3D, 74, 15, 25B) show trends similar to those in Alkaline series 1. In Alkaline series 1 the rocks containing such amphiboles are alkali-feldspar syenites; in Alkaline series 2 they are alkali-feldspar granites.

In Alkaline series 2, each individual crystal is much more homogeneous in composition than in Alkaline series 1 (spots 1–7, sample 51, Fig. 5c; analyses locations in Fig. 4e). For instance, the conspicuous core–rim trends, characteristic of the amphiboles in Alkaline series 1, are much less pronounced in the calcic amphiboles and completely lack in the sodic–calcic amphiboles. A progressive reduction in the occupancy of the A site with increasing Si is observed (Fig. 3b) and amphiboles vary systematically towards more sodic compositions (Fig. 5c) as alkalinity increases (Fig. 6b). However, the identification of the two groups of Giret et al. (1980) is less obvious (Fig. 3b), and the compositional gap between them is much more subtle (Fig. 6b). One exception to this pattern is sample 49 — the only sample with primary sodic amphibole. It shows compositions that grade into arfvedsonite (Fig. 3b), and record decreasing alkalinity (Fig. 6b).

Post-magmatic transformations in Alkaline series 2 are similar to those observed in Alkaline series 1, and are particularly pronounced in the samples with sodic–calcic amphiboles (e.g., sample 51, Fig. 4e, f). The

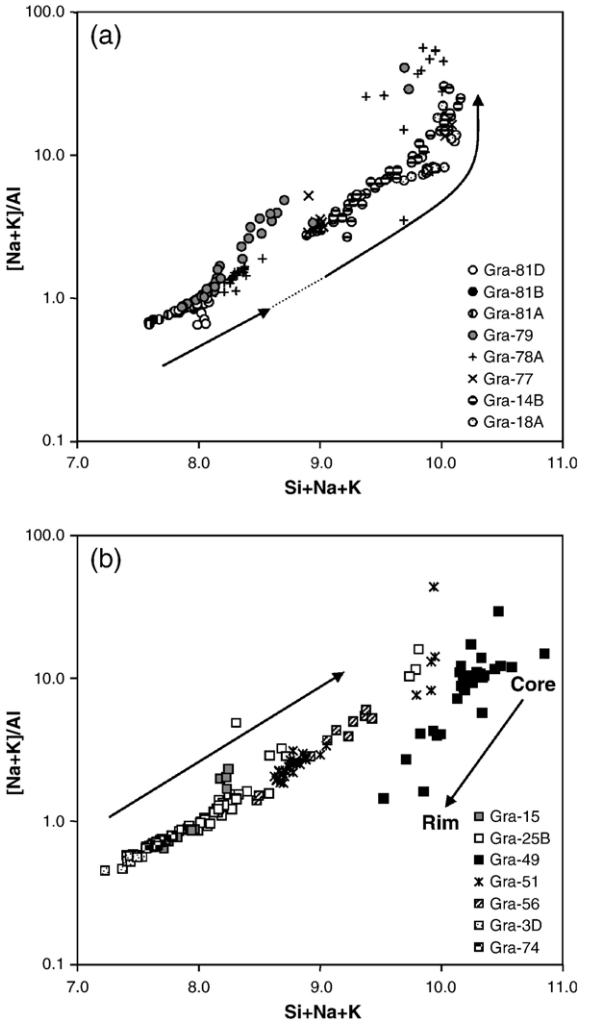


Fig. 6. (Si+Na+K) vs. [Na+K]/Al cationic plots (after Giret et al., 1980) for amphiboles of the (a) Alkaline series 1 and (b) Alkaline series 2. A trend of increasing alkalinity ([Na+K]/Al) is seen in both cases (arrows indicate core-to-rim trends), but at high alkalinity the two associations differ, with a tendency toward stronger increase in alkalinity in Alkaline series 1.

riebeckite crystals in sample 51 (Fig. 3b) are found as overgrowths (spots 22, 23, Fig. 4f and 5c) or fringes of acicular crystals (spots 8, Figs. 4e and 5c), usually developed on the margins of the amphibole crystals.

4.2. Biotite

Biotite in these rocks is unique in both textural and compositional terms. In Alkaline series 1, biotite is pleochroic in shades of deep red, while in Alkaline series 2 shades of beige are seen. Most commonly, biotite is present as irregular, radiated or fibrous aggregates in close association with needle-like riebeckite or grunerite (Figs. 4d, and 7a, b). Very rarely, red biotite is present as isolated crystals in the Alkaline series 1 (Fig. 7c). Textural features suggest that biotite formed under post-magmatic conditions concomitantly with post-magmatic sodic amphibole.

Compositionally, the biotites are rich in the annite molecule, with high Fe/[Fe+Mg] ratios and varying ^{IV}Al contents (Appendix C, Fig. 8). Biotites in Alkaline series 1 are characterized by Fe/[Fe+Mg] ratios close to 1, while those in the Alkaline series 2 show Fe/[Fe+Mg] ratios close to 0.9. Moreover, the abundance of ^{IV}Al is clearly more varying in Alkaline series 2. In both cases, ^{IV}Al values lower than 2 are common. In the biotites of Alkaline series 2, ^{IV}Al values occasionally reach values more typical of conventional biotites, especially those in sample 15. The low and varying ^{IV}Al values seen in two of the samples (25B, 59A) are at least partly caused by low occupancy of the K sites, associated with low total sums of the analyses (~ 90 wt.%). This suggests that the variability is related to alteration, and is not characteristic of the original biotite. Besides the variations in ^{IV}Al, variations in Ti (a substitute for divalent cations in the octahedral positions) are also important. As expected, ^{VI}Al is absent in most of the samples (Appendix C).

5. Discussion

5.1. Magmatic evolution of amphibole

5.1.1. Alkaline series 1

The existence of two groups of amphiboles (one characterized by calcic and sodic–calcic amphiboles; another composed of mostly sodic amphiboles) was first identified by Giret et al. (1980), and is very well illustrated by the amphiboles of the Alkaline series 1. The gap between the two groups is even more pronounced if only core compositions are considered. To some extent, this gap may represent a sampling bias in our dataset, but it may also bear significance to the stability of sodic–calcic amphiboles, as speculated by Giret et al. (1980).

The zoning patterns in amphiboles from this series are quite conspicuous, with the cores following an intermediate trend in Fig. 3a. Variations along this line can be explained by tschermakitic substitutions (cf. Giret et al., 1980; Njonfang and Moreau, 2000) and the trends recorded by the cores of the calcic to sodic–calcic amphiboles and the sodic amphiboles parallel those observed in the Zomba-Malosa granites (Woolley and Jones, 1992) and the Newfoundland granites (Strong and Taylor, 1984), respectively. The examples presented here, however, document this variability quite clearly. Strong and Taylor (1984) concluded that trends of this

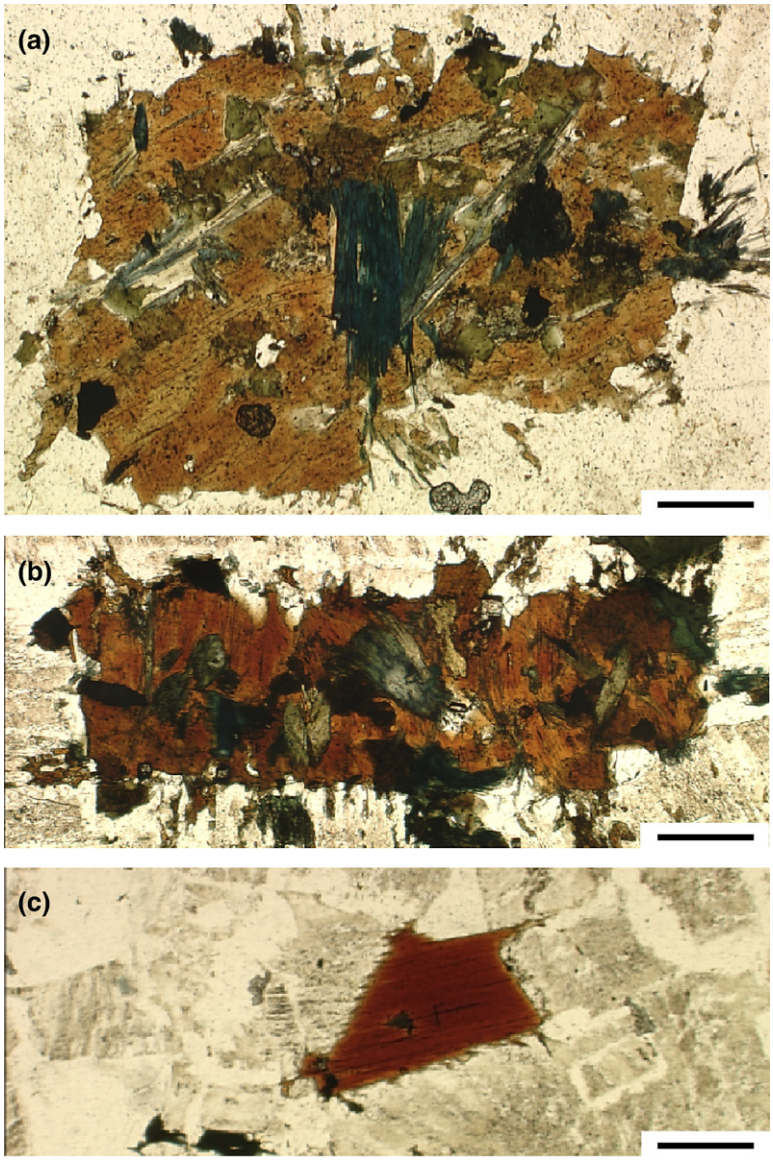


Fig. 7. Photomicrographs of biotite textures. (a and b) Intergrowth of red biotite and navy-blue amphibole in the Alkaline series 1, probably formed after primary sodic–calcic amphibole; bars correspond to 300 μm. (c) Isolated crystal of red biotite in the Alkaline series 1; the composition of this grain is undistinguishable from those illustrated in (a) and (b); bar corresponds to 450 μm. Plain-polarized light.

kind are characteristic of the magmatic to subsolidus evolution of amphiboles. The trend of the core compositions in Alkaline series 1 (Fig. 3a) shows that they can be related to each other by simple tschermakitic substitution, complying with the hypothesis of a comagmatic series. Interestingly, if the samples in this series were related by simple differentiation mechanisms (e.g., fractional crystallization), this must have happened at a stage when only the cores of the amphiboles had crystallized, given the diverging rim compositions. In other words, the observed inter-sample variability must have been imposed early in the magmatic evolution (i.e., in the early-magmatic stage).

The rims of the amphiboles in this series record compositional variations that diverge from the intermediate line and approach the lower line in Fig. 3a. This pattern is due to a decrease in the $[Na+K]_A$ content with increasing Na_B value. Variations like these cannot be explained by edenitic or tschermakitic substitutions. In this sense, each sample shows an independent (but analogous) evolution. Trajectories like these have been attributed to magmatic oxidation (Strong and Taylor,

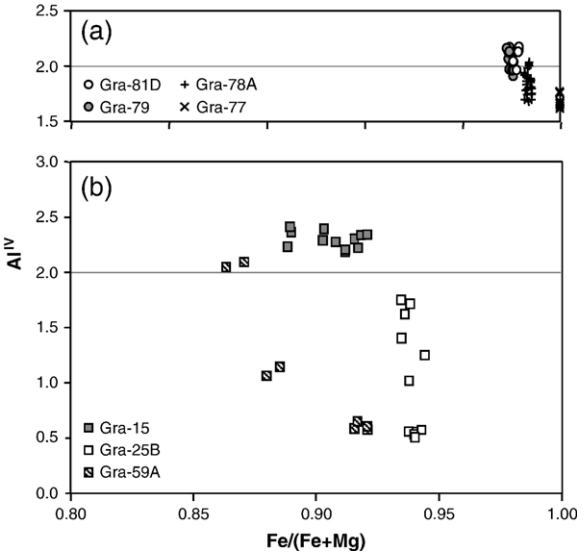


Fig. 8. ^{IV}Al vs. Fe/(Fe+Mg) cationic plots for biotites of Alkaline series 1 (a) and Alkaline series 2 (b) of the Serra da Graciosa A-type Granites and Syenites. Biotite in these rocks is highly enriched in Si, a characteristic feature of biotites coexisting with sodic amphibole (see text); those in the Alkaline series 1 are particularly rich in Fe as well. Part of the variation in ^{IV}Al in the Alkaline series 2 is due to alkali loss.

1984; Della Ventura et al., 2005) and can be explained by a substitution mechanism of the type

$$[Na, K]^A + [Fe^{2+}]^C \Leftrightarrow [\square]^A + [Fe^{3+}]^C \quad (1)$$

Direct testing of the suitability of this substitution mechanism is hampered by the dependency of the Fe^{3+} values on the mineral formula calculation procedure (cf. Gualda and Vlach, 2005). However, the lack of correlation between the variations in $[Na+K]_A$ and Si suggests that this substitution mechanism is indeed responsible for the variations seen. In this sense, the rims of the amphiboles illustrate a second stage of evolution of these amphiboles, characterized by crystallization under progressively more oxidizing conditions at the late-magmatic stage.

Another noteworthy aspect of the compositional trends observed is the variation in the [Na+K]/Al ratio. Giret et al. (1980) showed that a direct relationship exists between [Na+K]/Al ratios of amphiboles and the agpaitic index ($Al = \{[Na_2O+K_2O]/Al_2O_3\}_{mol}$) of the rocks in which they are found. They further demonstrated that the [Na+K]/Al ratio varies widely in amphiboles from peralkaline rocks, recording variations in alkalinity in the crystallizing melt. Our results, in particular the concomitant increase in Na_B and [Na+K]/Al, clearly support this conclusion. The compositional variations seen indicate increasing alkalinity within a given sample as the magma solidified, but also the simultaneous increase in alkalinity and silica supersaturation for the series as a whole, as also seen in the granites from Zomba-Malosa (Woolley and Jones, 1992).

5.1.2. Alkaline series 2

In Alkaline series 2, variations within each sample are relatively restricted and zoning patterns are subtle. The observed compositions fall along a single trend occupying the entire spectrum of calcic to sodic compositions and characterized by a gradually decreasing $[Na+K]_A$ sum with differentiation. This pattern is distinct from what is observed in the Alkaline series 1, and has not been reported before (cf. Figs. 3b and 2b–d).

The evolution of the amphiboles of the two alkaline series is similar in that Na (particularly Na_B) and Fe^{3+} contents and the [Na+K]/Al ratio increase with differentiation. This coupling between Na and Fe^{3+} indicates high alkalinity of the magmas from which the most sodic amphiboles crystallized. In fact, the [Na+K]/Al ratios of the primary sodic amphiboles in both associations are characteristic of agpaitic rocks (Giret et al., 1980). Only rocks with primary sodic amphibole are truly agpaitic and thus the textural distinction between magmatic and post-magmatic amphibole is of significance (see Section 4). This coupling between Na and Fe^{3+}— also identified by Czamanske and Dillet (1988) — is typical of pyroxenes of undersaturated agpaitic rocks, which reinforces the idea that these amphiboles crystallized in environments characterized by high alkalinity.

An exception to this pattern is sample 49 in the Alkaline series 2. It has cores of sodic amphibole characterized by low A-site occupancies and these evolve into amphiboles close to arfvedsonite end-member compositions. Thus there is a progressive increase in the A-site occupancy, favoring the left side of Eq. (1). This implies gradually more reducing conditions during the evolution of the sodic amphiboles, accompanied by a decrease in the degree of alkalinity of the magma, as indicated by the [Na+K]/Al ratios. Trends like this, which mark a stage of pronounced increase in alkalinity followed by a subtle decrease in alkalinity, are commonly observed in agpaitic series (cf. Khomyakov, 1995 and references therein), and reinforce the similarity between the evolution of the silica-oversaturated series described here and silica-undersaturated agpaitic series in general.

5.2. Post-magmatic transformations

Textural and compositional arguments strongly suggest that sodic amphibole forms in the post-

magmatic stage as overgrowths or as radiating aggregates or fringes that partly or entirely substitute primary amphibole. These transformations are most pronounced in varieties with primary sodic–calcic amphibole. Giret et al. (1980) suggested that the compositional gap between sodic–calcic and sodic amphiboles is due to the destabilization of sodic–calcic amphiboles caused by increasing alkalinity. This suggestion finds support in our observations, which indicate that samples with primary sodic–calcic amphibole most frequently include post-magmatic sodic–calcic or sodic amphibole, separated from the magmatic amphiboles by a compositional gap.

Post-magmatic sodic amphibole is always accompanied by Fe-rich, Al-poor varieties of biotite. Micas like these are sometimes referred to as "tetrasilicic" (cf. Robert and Maury, 1979; Czamanske and Dillet, 1988), due to the high Si contents in the tetrahedral sites; the use of this name, however, was discouraged by Rieder et al. (1998). In any case, micas like these are extremely rare, and their occurrence seems to be limited to cases where they coexist with sodic amphiboles (Robert and Maury, 1979; Czamanske and Dillet, 1988). In the manganesiferous commendites studied by Robert and Maury (1979), the tetrahedral Si contents are in some cases larger than 7. It is noteworthy that in the peralkaline porphyries described by Czamanske and Dillet (1988), the biotites are regarded as alteration products of primary amphibole. We speculate that the origin of "tetrasilicic" biotite is intrinsically related to the breakdown of sodic–calcic amphiboles and formation of sodic amphibole and biotite under subsolidus conditions.

6. Conclusions

The data presented here allows the recognition of differentiation trends for the amphiboles present in two alkaline series of the Serra da Graciosa A-type Granites and Syenites. Amphiboles in both series are characterized by increasing Na and Fe^{3+} values, which reflects the increasing alkalinity of the evolving magmas, a pattern very akin to that observed in mafic minerals in undersaturated agpaitic felsic rocks.

Alkaline series 1 is characterized by alkali-feldspar syenites and granites that show amphibole compositions grading towards more sodic varieties with increasing quartz abundance and decreasing mafic mineral contents. The evolutionary trends of amphiboles in these rocks are characterized by two main growth stages: (1) the cores of the crystals form a trend characterized by increasing Na_B and Fe^{3+} and almost constant $(Na+K)_A$ values close to 0.5 pfu, which corresponds to the main differentiation stage; (2) the rims of the amphiboles show a marked decrease in $(Na+K)_A$, which is observed irrespective of the core compositions, and can be interpreted to represent conditions of increasing oxidation during the final stages of magmatic crystallization. A compositional gap exists between sodic–calcic amphiboles, and may be due to the destabilization of amphibole at a particular degree of alkalinity, as originally suggested by Giret et al. (1980).

Amphibole from Alkaline series 2 shows different traits. Individual grains are less strongly zoned and no clear distinction in the evolution of rims and cores could be detected. The group of samples as a whole forms a single trend, characterized by a slight decrease in $(Na+K)_A$ values of calcic amphiboles and a marked increase towards arfvedsonitic compositions for the sodic amphiboles. The pronounced increase in $(Na+K)_A$ in primary sodic amphiboles is indicative of progressively more reducing conditions in the more differentiated varieties of this series.

In both cases, subsolidus transformations are common, particularly in the rocks bearing sodic–calcic amphibole, which breaks down and is replaced by intergrowths of Al-poor ("tetrasilicic") biotite and acicular sodic amphibole.

Acknowledgements

G. Gualda benefited from a M.Sc. scholarship from FAPESP (Fundação de Amparo à Pesquisa do Estado de São Paulo, Brazil) during part of the duration of the project. We are indebted to Laura Lauri, and Torkil Røhr for detailed reviews of the original manuscript. Careful editorial handling by Tapani Rämö helped improve the manuscript significantly, and is much appreciated.

Appendix A. Supplementary data

Supplementary data associated with this article can be found, in the online version, at doi:10.1016/j.lithos.2006.03.070.

References

Barker, F., Wones, D.R., Sharp, W.N., Desborough, G.A., 1975. Pikes Peak Batholith, Colorado Front Range, and model for origin of gabbro–anorthosite–syenite–potassic granite suite. Precambrian Research 2, 97–160.

Bastin, G.F., Heijligers, H.J.M., 1990. Progress in electron-probe microanalysis. Materialwissenschaft und Werkstofftechnik 21, 90–92.

Carmichael, I.S.E., Turner, F.J., Verhoogen, J., 1974. Igneous Petrology. McGraw-Hill, New York.

Czamanske, G.K., Dillet, B., 1988. Alkali amphibole, tetrasilicic mica, and sodic pyroxene in peralkaline siliceous rocks, Questa Caldera, New Mexico. American Journal of Science 288A, 358–392.

Deer, W.A., Howie, R.A., Zussman, M.A., 1992. An Introduction to the Rock-Forming Minerals, 2nd edition. Longman, London.

Deer, W.A., Howie, R.A., Zussman, M.A., 1997. 2nd edition. Rock-Forming Minerals, Double-Chain Silicates, vol. 2B. The Geological Society, London.

Della Ventura, G., Iezzi, G., Redhammer, G.J., Hawthorne, F.C., Scaillet, B., Novembre, D., 2005. Synthesis and crystal-chemistry of alkali amphiboles in the system Na_2O–MgO–FeO–Fe_2O_3–SiO_2–H_2O as a function of f_{O2}. American Mineralogist 90, 1375–1383.

Giret, A., Bonin, B., Leger, J.-M., 1980. Amphibole compositional trends in oversaturated and undersaturated alkaline plutonic ring-complexes. Canadian Mineralogist 18, 481–495.

Gualda, G.A.R., Vlach, S.R.F., 2005. Stoichiometry-based estimates of ferric iron in calcic, sodic–calcic and sodic amphiboles, a comparison of various methods. Anais da Academia Brasileira de Ciências 77, 521–534.

Gualda, G.A.R., Vlach, S.R.F., submitted for publication. The Serra da Graciosa A-type Granites, southern Brazil. Part 1. Regional setting and geological characterization. Anais da Academia Brasileira de Ciências.

Gualda, G.A.R., Vlach, S.R.F., 2006. The Serra da Graciosa A-type Granites and Syenites, southern Brazil Part 2: Petrographic and mineralogical evolution of the alkaline and aluminous associations. Lithos 93, 310–327 (this issue). doi:10.1016/j.lithos.2006.06.002.

Hoshino, M., 1986. Amphiboles and coexisting ferromagnesian silicates in granitic-rocks in Mahé, Seychelles. Lithos 19, 11–25.

Jarosewich, E., Nelen, J.A., Norberg, J.A., 1980. Reference samples for electron microprobe analysis. Geostandards Newsletter 4, 43–47.

Kaul, P.F.T., Cordani, U.G., 2000. Geochemistry of the Serra do Mar (southern Brazil) granitoid magmatism and tectonic implications. Revista Brasileira de Geociências 30, 115–119.

Khomyakov, A.P., 1995. Mineralogy of Hyperagpaitic Alkaline Rocks. Oxford University Press, New York.

King, P.L., White, A.J.R., Chappel, B.W., Allen, C.M., 1997. Characterizations and origin of aluminous A-type granites from the Lachlan Fold Belt, Southeastern Australia. Journal of Petrology 38, 371–391.

Leake, B.E., Woolley, A.R., Arps, C.E.S., Birch, W.D., Gilbert, M.C., Grice, J.D., Hawthorne, F.C., Kato, A., Kisch, H.J., Krivovichev, V.G., Linthout, K., Laird, J., Mandarino, J.A., Maresch, W.V., Nickel, E.H., Rock, N.M.S., Schumacher, J.C., Smith, D.C., Stephenson, N.C.N., Ungaretti, L., Whittaker, E.J.W., Youzhi, G., 1997. Nomenclature of amphiboles: report of the Subcommittee on Amphiboles of the International Mineralogical Association, Commission on New Minerals and Mineral Names. Mineralogical Magazine 61, 295–321.

Marks, M., Vennemann, T., Siebel, W., Markl, G., 2003. Quantification of magmatic and hydrothermal processes in a peralkaline syenite–alkali granite complex based on textures, phase equilibria, and stable and radiogenic isotopes. Journal of Petrology 44, 1247–1280.

Neumann, E.-R., 1976. Compositional relations among pyroxenes, amphiboles and other mafic phases in the Oslo Region plutonic rocks. Lithos 9, 85–109.

Njonfang, E., Moreau, C., 2000. The mafic mineralogy of the Pandé massif, Tikar plain, Cameroon, implications for a peralkaline affinity and emplacement from highly evolved alkaline magma. Mineralogical Magazine 64, 525–537.

Parsons, I., 1981. The Klokken Gabbro–Syenite Complex, South Greenland: quantitative interpretation of mineral chemistry. Journal of Petrology 22, 233–260.

Pitcher, W.S., 1997. The Nature and Origin of Granite, 2nd edition. Blackie Academic and Professional, London, pp. 258–279.

Platt, R.G., Woolley, A.R., 1986. The mafic mineralogy of the peralkaline syenites and granites of the Mulanje Complex, Malawi. Mineralogical Magazine 50, 85–99.

Rieder, M., Cavazzini, G., D'Yakonov, Y.S., Frank-Kamenetskii, V.A., Gottardi, G., Guggenheim, S., Koval, P.V., Muller, G., Neiva, A.M.R., Radoslovich, E.W., Robert, J.L., Sassi, F.P., Takeda, H., Weiss, Z., Wones, D.R., 1998. Nomenclature of the micas. Canadian Mineralogist 36, 905–912.

Robert, J.-L., Maury, R.C., 1979. Natural occurrence of a (Fe, Mn, Mg) tetrasilicic potassium mica. Contributions to Mineralogy and Petrology 68, 117–123.

Schumacher, J.C., 1997. Appendix 2, the estimate of ferric iron in electron microprobe analysis of amphiboles. Canadian Mineralogist 35, 238–246.

Shand, S.J., 1972. Eruptive Rocks, 4th edition. John Willey and Sons, New York, pp. 225–245.

Siga Jr., O., Basei, M.A.S., Machiavelli, A., 1993. Evolução geotectônica da porção NE de Santa Catarina e SE do Paraná, com base em interpretações geocronológicas. Revista Brasileira de Geociências 23, 215–223.

Strong, D.F., Taylor, R.P., 1984. Magmatic-subsolidus and oxidation trends in composition of amphiboles from silica-saturated peralkaline igneous rocks. Tschermaks Mineralogische und Petrographische Mitteilungen 32, 211–222.

Woolley, A.R., Jones, G.C., 1992. The alkaline/peralkaline syenite-granite complex of Zomba-Malosa, Malawi, mafic mineralogy and genesis. Journal of African Earth Sciences 14, 1–12.